partially by upregulation of perforin and granzyme B, and that heat treatment of CTLs at 41 °C abrogates CTL functions partially by inducing apoptosis. Augmentation of CTL functions by heat treatment might be one significant reason of fever induced by inflammation and also one mechanism of hyperthermia.

Materials and methods

Cells and antibodies

T2-A24 cells, human leukocyte antigen (HLA)-A24 gene-transduced T2 cells, were a kind gift from Dr. K. Kuzushima (Nagoya, Japan). The cells were cultured in RPMI1640 (SIGMA) supplemented with 10 % FBS (Life Technologies) and 800 μg/ml of G418 (Life Technologies). K562 cells were obtained from ATCC and cultured in RPMI1640 supplemented with 10 % FBS. The antibodies used in this study are summarized in Table 1.

Establishment of CTL clone #IM29

A survivin peptide-specific CTL clone was established from peripheral blood of a 44-year-old patient with rectal carcinoma who was treated with survivin peptide immunization and IFNα (Kameshima et al. 2011). Survivin peptide-specific CTLs were stained with survivin peptide-HLA-A24 complex tetramer and were single-cell-sorted by FACS Aria II (BD) into a round-bottomed 96-well plate at single cell per well. The CTL was incubated with irradiated 8×10^4 peripheral blood mononuclear cells (PBMCs) in AIM-V (Life Technologies) medium supplemented with 10 % human AB serum (kindly provided by Dr. Tatsuo Usui, Hokkaido Red

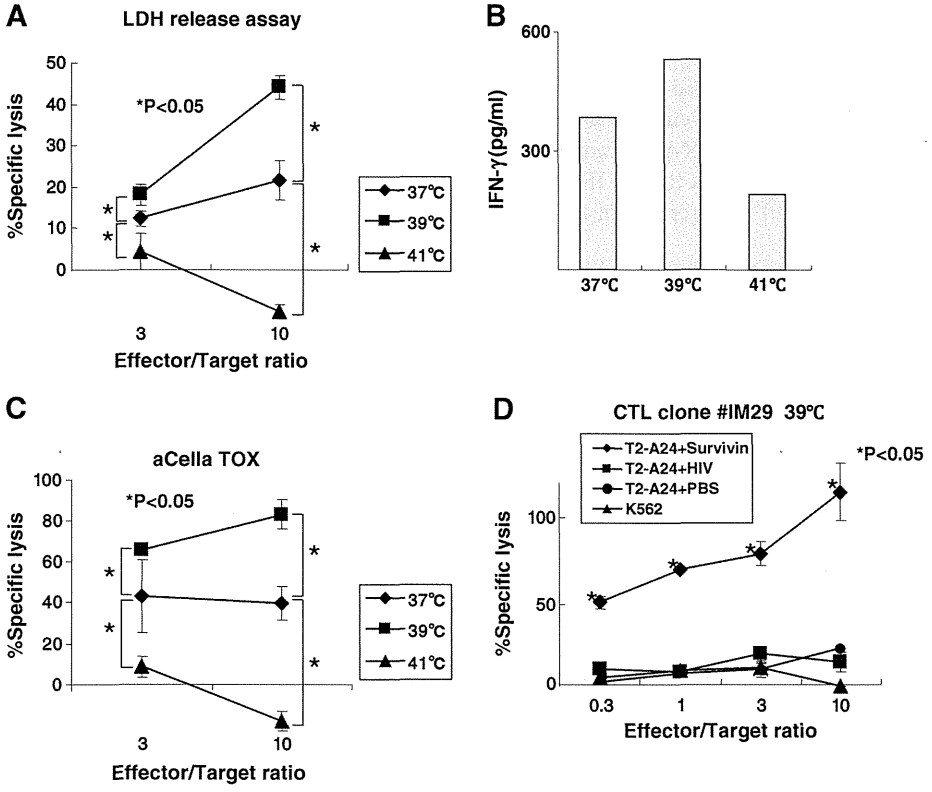

Fig. 2 Heat treatment enhances CTL functions. **a** Cytotoxicity of CTL clone #IM29 in several temperature conditions. Cytotoxicity of CTL clone #IM29 using T2-A24 cells pulsed with survivin peptide was evaluated by LDH release assay under several temperature conditions (37, 39, and 41 °C). *Asterisks* represent significant difference ($P<0.05$, *t* test). Data are mean±SD. **b** IFN-γ secretion of CTL clone #IM29 in several temperature conditions. IFN-γ secretion of CTL clone #IM29 using T2-A24 cells pulsed with survivin peptide was evaluated by ELISA under several temperature conditions (37, 39, and 41 °C). Data are mean. **c** Cytotoxicity of CTL clone #IM29 using aCella TOX assay. Cytotoxicity of CTL clone #IM29 using T2-A24 cells pulsed with survivin peptide was evaluated by aCella TOX assay under several temperature conditions (37, 39, and 41 °C). *Asterisks* represent significant difference ($P<0.05$, *t* test). Data are mean ± SD. **d** Cytotoxicity of CTL clone #IM29 in 39 °C condition. CTLs were preincubated in 39 °C for 1 day before cytotoxicity assay. Cytotoxicity of CTL clone #IM29 was evaluated with survivin peptide-pulsed T2-A24 cells, control peptide (HIV)-pulsed T2-A24 cells and K562 cells in 39 °C. *Asterisks* represent significant difference compared with HIV peptide-pulsed T2-A24 cells or K562 cells ($P<0.05$, *t* test). Data are mean±SD

Cross Blood Center, Sapporo, Japan), 200 IU of IL-2 (R&D Systems), and 5 μg/ml of PHA (SIGMA). Growing wells were transferred into a 24-well plate and fed every 3 days with AIM-V supplemented with 10 % human AB serum and 200 IU of IL-2. On day 34, clones were assessed by survivin tetramer staining and HIV-tetramer as a negative control (Fig. 1a). Tetramers were obtained from MBL Co., Ltd. (Nagoya, Japan).

Cytotoxicity assay and IFN-γ ELISA

CTL clone #IM29 were preincubated at 37–41 °C for 1 day before cytotoxicity assay and IFN-γ ELISA. Survivin peptide-pulsed T2-A24 cells were seeded into a 96-well plate at 5×10^3 cells/well. CTL clone #IM29 cells were seeded at several effector/target (*E*/*T*) ratios, then incubated at 37–41 °C for 6 h. Cytotoxicity of CTL clone #IM29 cells was examined by using an LDH cytotoxicity detection kit (TAKARA BIO Inc., Osaka, Japan) and aCella TOX kit (Cell Technology, Inc., Mountain View, CA) according to the manufacturer's protocol.

Ten thousand survivin peptide-pulsed T2-A24 cells and 3×10^3 of CTL clone #29 cells were co-cultured in a 96-well plate at 37–41 °C for 12 h, and then IFN-γ concentrations in supernatants were measured by using a Human IFN gamma ELISA Kit (Thermo Scientific) as described in the manufacturer's protocol.

Live images of cytotoxicity were recorded by the OLYMPUS FLUOVIEW FV 300-I71BG-SP system (OLYMPUS). Briefly, T2-A24 cells were transduced with GFP-plasmid using a Nucleofector V kit (Amaxa). GFP-positive T2-A24 cells were pulsed with survivin peptide and co-cultured with CTL clone #IM29 cells at an *E*/*T* ratio=10, and cultured in 37–41 °C for 4 h and live image were recorded.

Flow cytometry

For detection of HLA-A24 of T2-A24 cells, T2-A24 cells were stained with anti-HLA-A24 mAb (C7709A2.6, kind gift from Dr. P. G. Coulie, Brussels, Belgium) for 1 h, washed three times with PBS, stained with FITC-labeled anti-mouse IgG+M antibody (KPL, 200 times dilution) for 30 min, and washed again one time with PBS. T2-A24 cells were analyzed by a FACS Calibur (BD).

After treatment of CTL clone #IM29 cells at 37–41 °C for 12 h, the expression of CD3, CD8, and TCRαβ was examined by ad FACS Calibur. After staining with first antibodies (summarized in Table 1), CTL clone #IM29 cells were stained with FITC-labeled anti-mouse IgG+M antibody and then analyzed by a FACS Calibur. Mean fluorescent intensity was calculated by CELL Quest software (BD).

Western blot

Western blot analysis was performed as described previously (Nakatsugawa et al. 2011). Anti-perforin, granzyme B, Fas ligand, HSP90, and β-actin mAbs were used at 1,000×, 1,000×, 1,000×, 1,000×, and 2,000× dilutions, respectively (summarized in Table 1). The specific bands were quantified by using Image J software (NIH).

Detection of apoptosis

Apoptotic cells were detected by staining with anti-annexin V antibody and propidium iodide (PI) using annexin V FLUOD staining kit (Roche) according to the manufacturer's protocol and then analyzed by a FACS Calibur. For detection of dead cells, CTLs were stained with Trypan Blue (Life Technologies) and % dead cells were calculated by Countess Automated Cell Counter (Life Technologies). Caspase-3 activity was measured by using APOPCYTO Caspase-3 Colorimetric Assay Kit (MBL, Nagoya, Japan) according to the manufacturer's protocol. CTLs were preincubated under 37–41 °C conditions for 24 h, before caspase-3 assay.

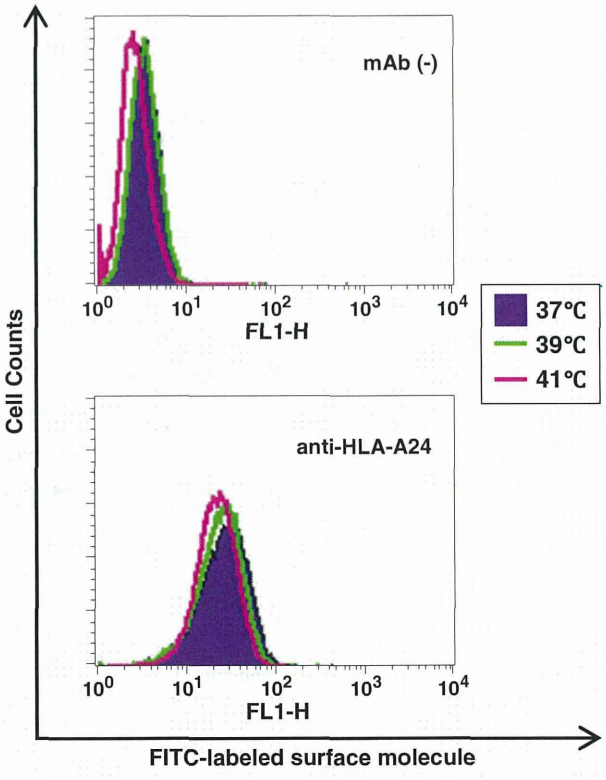

Fig. 3 Heat shock did not alter HLA-A24 expression on T2-A24 cells. The expression of HLA-A24 on T2-A24 cells under several temperature conditions was evaluated by a FACS Calibur. Mean fluorescent intensity (MFI) are listed in ESM 5

Results

Establishment of survivin-derived antigenic peptide-specific CTL clone

To establish a CTL clone specific for cancer cells, we sorted survivin peptide-specific CTLs using survivin peptide-HLA-A24 complex tetramer (Fig. 1a). Sorted CTLs were grown in 96-well plates and a survivin tetramer-positive CTL clone (#IM29) was established (Fig. 1a). CTL clone #IM29 recognized survivin peptide-pulsed T2-A24 cells at different *E*/*T* ratios, whereas it did not recognize control peptide-pulsed T2-A24 cells or K562 cells, indicating that CTL clone #IM29 is specific for survivin peptide (Fig. 1b).

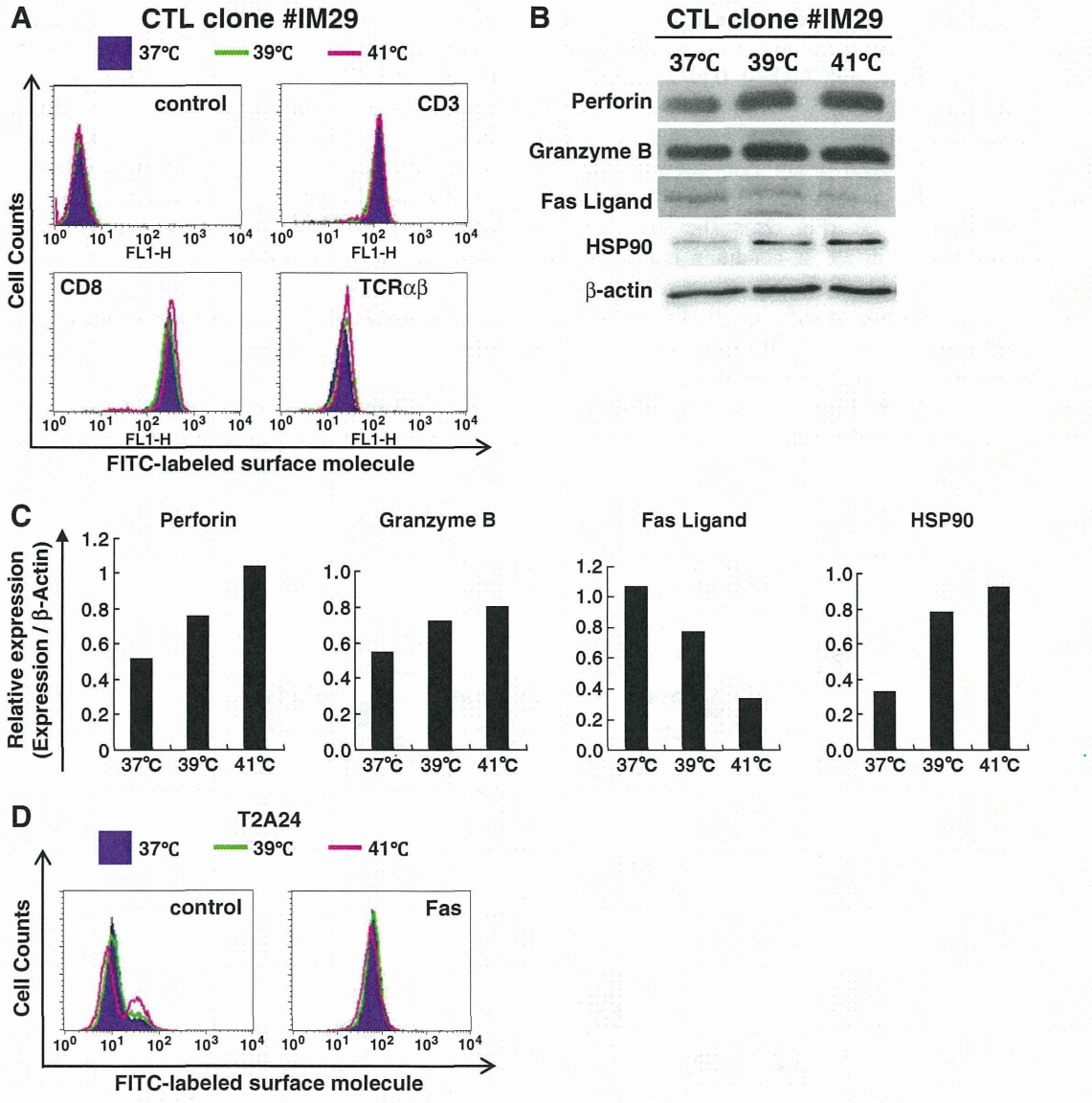

Fig. 4 Expression of several molecules of CTL in several temperature conditions. **a** Flow cytometer analysis of surface molecules on CTL clone #IM29 cells under several temperature conditions. CD3, CD8 and TCRαβ expression on CTL clone #IM29 under several temperature conditions was analyzed by using a flow cytometer. Mean fluorescent intensity (MFI) are listed in ESM 6. **b** Western blot analysis of CTL clone #IM29 under several temperature conditions. Perforin, granzyme B, Fas ligand and HSP90 protein expression in CTL clone #IM29 under several temperature conditions was analyzed by western blot analysis. β-Actin was uses as a internal positive control. Data are representative Western Blot pictures. **c** Quantification of protein expression in CTL clone #IM29 under several temperature conditions. Western blot bands were analyzed, and quantified by Image J software (NIH). Perforin, granzyme B, Fas ligand, and HSP90 expression were standardized by β-Actin. Data are relative expression of perforin, granzyme B, Fas ligand and HSP90. **d** Heat shock did not alter Fas expression on T2-A24 cells. The expression of Fas on T2-A24 cells under several temperature conditions was evaluated by a FACS Calibur. Mean fluorescent intensity (MFI) are listed in ESM 7

Heat treatment enhanced CTL functions

To address the effects of heat treatment on CTL functions, we evaluated CTL functions under several temperature (37–41 °C) conditions (Fig. 2a, b, c and Electronic supplementary material (ESM)). Cytotoxicity of CTL was significantly enhanced in 39 °C condition compared with 37 °C condition, whereas the cytotoxicity was decreased in 41 °C condition by LDH release assay (Fig. 2a). IFN-γ secretion also showed similar pattern as cytotoxicity with highest IFN-γ secretion in 39 °C condition (Fig. 2b). To confirm the cytotoxicity results using LDH release assay, we performed aCella TOX assay. aCella TOX assay also showed that the cytotoxicity of CTL was greatest in 39 °C condition, and minimum in 41 °C (Fig. 2c). The specificity of CTL was not altered in 39 °C condition indicating that heat shock enhances only antigenic peptide-specific cytotoxicity, but not non-specific cytotoxicity (Fig. 2d).

Heat shock induced the HSP70 expression in T2-A24 cells (Supplemental data 4), whereas the expression of HLA-A24 molecule on T2-A24 cells was not enhanced under heat shock conditions (Fig. 3).

Heat treatment upregulated the expression of perforin

CTLs recognize target cells through cell surface molecules, including CD3, CD8, and TCRαβ, and kill target cells by secretion of cytotoxic granule proteins including perforin and granzyme B. We investigated the expression of these molecules in CTLs under several temperature conditions (Fig. 4a and b). The expression of CD3, CD8, and TCRαβ on the surface of CTLs were almost the same in all temperature conditions (37–41 °C; Fig. 4a and b). On the other hand, the expression of perforin and granzyme B were enhanced in high temperature conditions (39 °C and 41 °C) compared with its expression in 37 °C condition (Fig. 4b and c). Fas ligand protein, another cytotoxic molecule expression and Fas expression on T2-A24 cells did not show any increase (Fig. 4b and d).

Heat treatment (41 °C) increased apoptotic cell death of CTLs

Since CTL activity was minimum in the condition of 41 °C, we investigated the cell conditions of CTLs in several

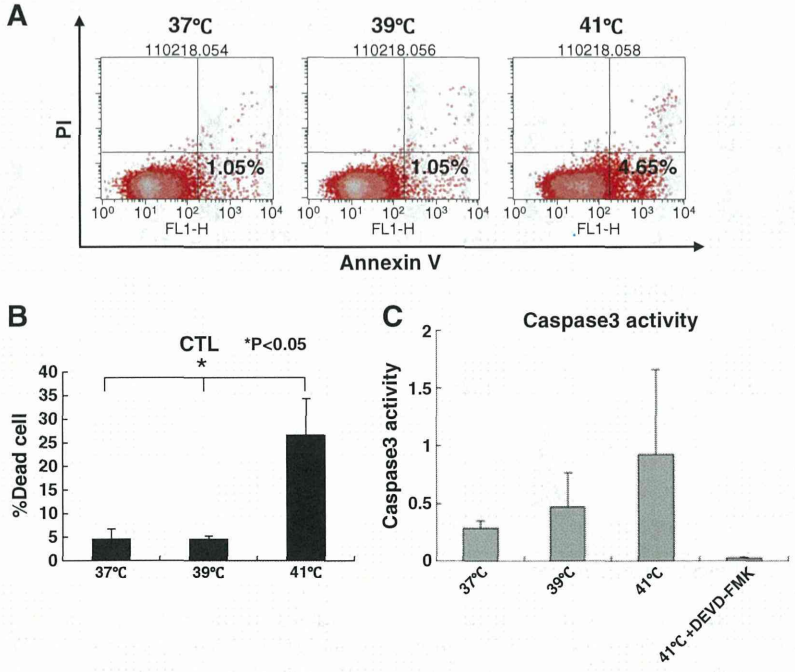

Fig. 5 Apoptotic cell death was induced under 41 °C condition. **a** Detection of apoptosis under several temperature conditions. Apoptotic cell death was detected by anti-annexin V and propidium iodide (PI) staining under several temperature conditions. Percentages represent apoptotic cells (annexin V-positive and PI-negative cells). **b** Percent dead cells was increased in 41 °C. CTLs were preincubated in 37–41 °C for 1 day. CTLs were stained with Trypan Blue and %dead cells were counted by Countess Automated Cell Counter. *Asterisks* represent significant difference ($P<0.05$, *t* test). Data are mean+SD. **c** Caspase 3 was activated in 41 °C. CTLs were preincubated in 37–41 °C for 1 day. Caspase 3 activities were measured by APOPCYTO Caspase-3 Colorimetric Assay Kit. Data are mean+SD

temperature conditions. Trypan Blue staining of CTLs cultured in several temperatures revealed that the percentage of dead cells was highest in 41 °C condition (Fig. 5b). To address the type of cell death, annexin V and PI staining was performed to detect apoptotic cell, which were greater at 41 °C than in other temperature conditions (Fig. 5a); and Caspase-3 activity was highest in the 41 °C condition (Fig. 5c). Thus, the CTL cell death partially by apoptosis under 41 °C condition might be the reason of low CTL activity in high temperature.

Discussion

The physiological meaning of fever caused by inflammation has been a major issue for a long time. In this study, we showed for the first time that CTL activity was upregulated by heat treatment. Results of the cytotoxicity assay and IFN-γ assay showed that CTL activity was greatest at 39 °C and that it was the minimum at 41 °C. These observations indicate that fever caused by systemic inflammatory cytokine release enhances CTL functions, and this might enhance eradication of pathogens. The enhancement of cytotoxicity might depend on upregulation of cytotoxic granule proteins including perforin and granzyme B. After secretion from CTLs, perforin is inserted into the plasma membrane, make pore and lyse target cells. Upregulation of cytotoxic granule proteins might not be involved in the enhancement of IFN-γ secretion, suggesting the existence of another molecular mechanism to enhance CTL functions by heat shock.

The exact molecular mechanisms by which cytotoxic granule proteins are upregulated in heat-treated CTLs remain unclear. Since we treated CTLs at 39 °C, it may be transcription enhanced due to the activation of heat shock factor-1 (HSF1); however, there is no HSF1-binding site (heat shock element) in the promoter region of perforin and granzyme B. (Pipkin et al. 2010) Another possible explanation is stabilization of perforin protein by heat treatment. Heat treatment induces upregulation of several chaperone proteins including HSPs by HSF1, and thus association with these chaperone proteins may stabilize and prolong the life span of cytotoxic granule proteins. Further analysis is needed to clarify the exact molecular mechanisms.

Hyperthermia is one treatment modality for cancers, but the exact mechanisms by which it works to suppress cancers remain unclear. Adaptive immune systems induced by antigenic peptides bound to HSPs might be mechanisms (enhancement of induction phase of CTL). In this study, we showed that heat treatment enhanced the cytotoxicity activity of CTLs (enhancement of effector phase of CTL). Therefore, heat treatment will enhance both induction and effector phases of adaptive immune system. These two mechanisms should act synergistically, and the adaptive immune system should have a role in hyperthermia.

In summary, we showed for the first time that heat treatment of CTLs enhanced CTL functions. Upregulation of cytotoxic granule proteins may play a role in this phenomenon. Enhancement of CTL functions by heat treatment might have a role in CTL functions in fever and hyperthermia.

Acknowledgments The authors thank Ms. E. Nakazawa for technical assistance. The authors thank Dr. Tatsuo Usui (Hokkaido Red Cross Blood Center, Sapporo, Japan) for the kind donation of human sera. The authors thank Dr. K. Kuzushima and Dr. P. G. Coulie for providing cells. This work was supported by Grants-in-Aid for Scientific Research from the Ministry of Education, Culture, Sports, Science and Technology of Japan (grant Nos. 16209013, 17016061 and 15659097) for Practical Application Research from the Japan Science and Technology Agency, and for Cancer Research (15-17 and 19-14) from the Ministry of Health, Labor and Welfare of Japan, Ono Cancer Research Fund (to N. S.) and Takeda Science Foundation (to Y. H.). This work was supported in part by the National Cancer Center Research and Development Fund (23-A-44).

Declaration of financial disclosure The authors have no financial conflict of interest.

References

Bachleitner-Hofmann T et al (2006) Heat shock treatment of tumor lysate-pulsed dendritic cells enhances their capacity to elicit antitumor T cell responses against medullary thyroid carcinoma. J Clin Endocrinol Metab 91:4571–4577

Bernheim HA et al (1979) Fever: pathogenesis, pathophysiology, and purpose. Ann Intern Med 91:261–270

Brusa D et al (2009) Immunogenicity of 56 degrees C and UVC-treated prostate cancer is associated with release of HSP70 and HMGB1 from necrotic cells. Prostate 69:1343–1352

Hirohashi Y et al (2002) An HLA-A24-restricted cytotoxic T lymphocyte epitope of a tumor-associated protein, survivin. Clin Cancer Res 8:1731–1739

Kameshima H et al (2011) Immunogenic enhancement and clinical effect by type-I interferon of anti-apoptotic protein, survivin-derived peptide vaccine, in advanced colorectal cancer patients. Cancer Sci 102:1181–1187

Nakatsugawa M et al (2011) SOX2 is overexpressed in stem-like cells of human lung adenocarcinoma and augments the tumorigenicity. Lab Invest 91:1796–1804

Pipkin ME et al (2010) The transcriptional control of the perforin locus. Immunol Rev 235:55–72

Sato N et al (2009) Molecular pathological approaches to human tumor immunology. Pathol Int 59:205–217

Sato A et al (2010) Melanoma-targeted chemo-thermo-immuno (CTI)-therapy using *N*-propionyl-4-*S*-cysteaminylphenol-magnetite nanoparticles elicits CTL response via heat shock protein–peptide complex release. Cancer Sci 101:1939–1946

Shi H et al (2006) Hyperthermia enhances CTL cross-priming. J Immunol 176:2134–2141

Torigoe T et al (2009) Heat shock proteins and immunity: application of hyperthermia for immunomodulation. Int J Hyperthermia 25:610–616

Genome-wide analysis of DNA methylation identifies novel cancer-related genes in hepatocellular carcinoma

Masahiro Shitani, Shigeru Sasaki, Noriyuki Akutsu, Hideyasu Takagi, Hiromu Suzuki, Masanori Nojima, Hiroyuki Yamamoto, et al.

Tumor Biology
Tumor Markers, Tumor Targeting and Translational Cancer Research

ISSN 1010-4283
Volume 33
Number 5

Tumor Biol. (2012) 33:1307-1317
DOI 10.1007/s13277-012-0378-3

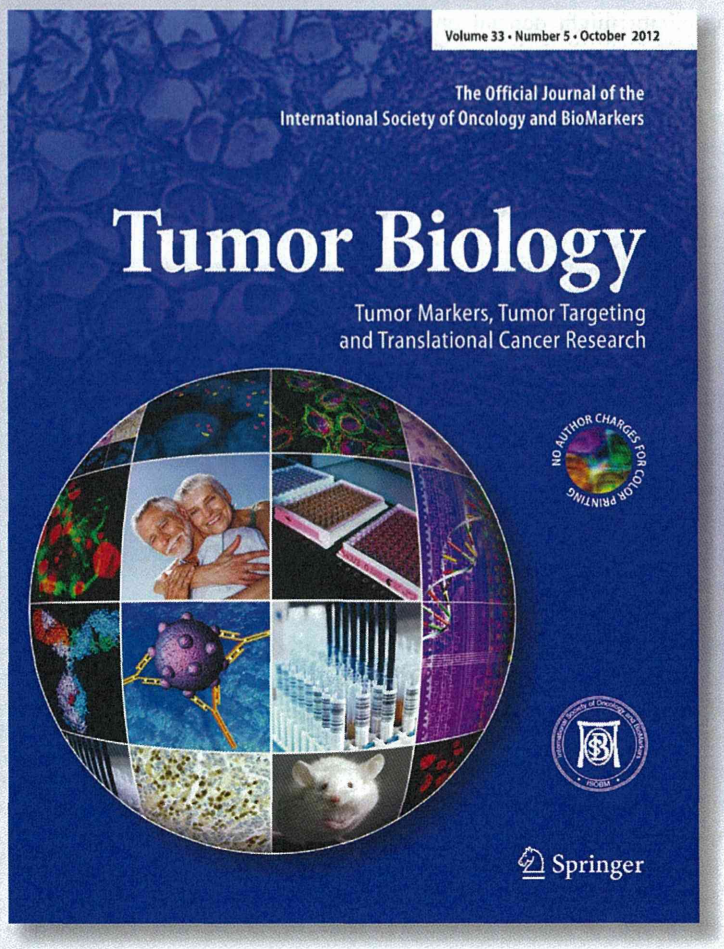

Springer

Tumor Biol. (2012) 33:1307–1317
DOI 10.1007/s13277-012-0378-3

RESEARCH ARTICLE

Genome-wide analysis of DNA methylation identifies novel cancer-related genes in hepatocellular carcinoma

Masahiro Shitani · Shigeru Sasaki · Noriyuki Akutsu · Hideyasu Takagi · Hiromu Suzuki · Masanori Nojima · Hiroyuki Yamamoto · Takashi Tokino · Koichi Hirata · Kohzoh Imai · Minoru Toyota · Yasuhisa Shinomura

Received: 24 January 2012 / Accepted: 11 March 2012 / Published online: 29 March 2012

Abstract Aberrant DNA methylation has been implicated in the development of hepatocellular carcinoma (HCC). Our aim was to clarify its molecular mechanism and to identify useful biomarkers by screening for DNA methylation in HCC. Methylated CpG island amplification coupled with CpG island microarray (MCAM) analysis was carried out to screen for methylated genes in primary HCC specimens [hepatitis B virus (HBV)-positive, $n=4$; hepatitis C virus (HCV)-positive, $n=5$; HBV/HCV-negative, $n=7$]. Bisulfite pyrosequencing was used to analyze the methylation of selected genes and long interspersed nuclear element (LINE)-1 in HCC tissue ($n=57$) and noncancerous liver tissue ($n=50$) from HCC patients and in HCC cell lines ($n=10$). MCAM analysis identified 332, 342, and 259 genes that were methylated in HBV-positive, HCV-positive, and HBV/HCV-negative HCC tissues, respectively. Among these genes, methylation of *KLHL35*, *PAX5*, *PENK*, and *SPDYA* was significantly higher in HCC tissue than in noncancerous liver tissue, irrespective of the hepatitis virus status. LINE-1 hypomethylation was also prevalent in HCC and correlated positively with *KLHL35* and *SPDYA* methylation. Receiver operating characteristic curve analysis revealed that methylation of the four genes and LINE-1 strongly discriminated between HCC tissue and noncancerous liver tissue. Our data suggest that aberrant hyper- and hypomethylation may contribute to a common pathogenesis mechanism in HCC. Hypermethylation of *KLHL35*, *PAX*, *PENK*, and *SDPYA* and hypomethylation of LINE-1 could be useful biomarkers for the detection of HCC.

Keywords Hepatocellular carcinoma · DNA methylation · CpG island · LINE-1 · Biomarker

Electronic supplementary material The online version of this article (doi:10.1007/s13277-012-0378-3) contains supplementary material, which is available to authorized users.

M. Shitani · S. Sasaki (✉) · N. Akutsu · H. Takagi · H. Suzuki · H. Yamamoto · Y. Shinomura (✉)
First Department of Internal Medicine,
Sapporo Medical University,
S1, W16, Chuo-Ku,
Sapporo 060-8543, Japan
e-mail: ssasaki@sapmed.ac.jp
e-mail: shinomura@sapmed.ac.jp

H. Suzuki · M. Toyota
Department of Molecular Biology, Sapporo Medical University,
Sapporo, Japan

M. Nojima
Department of Public Health, Sapporo Medical University,
Sapporo, Japan

T. Tokino
Medical Genome Science, Research Institute for Frontier Medicine, Sapporo Medical University School of Medicine,
Sapporo, Japan

K. Hirata
First Department of Surgery, Sapporo Medical University,
Sapporo, Japan

K. Imai
Division of Novel Therapy for Cancer, The Advanced Clinical Research Center, The Institute of Medical Science,
The University of Tokyo,
Tokyo, Japan

Introduction

Hepatocellular carcinoma (HCC) is one of the most common human malignancies, worldwide [1]. Chronic infection by hepatitis B virus (HBV) and hepatitis C virus (HCV) are well-documented risk factors for the development of HCC, while chronic alcoholism and various environmental factors, including aflatoxin B1, are also believed to be important risk

factors [2, 3]. The development and progression of HCC is often a complex, multistep process entailing the evolution of normal liver through chronic hepatitis and cirrhosis to HCC, but HCC can also arise in a noncirrhotic liver. In either case, the process is influenced by multiple genetic changes, including allelic deletions, chromosomal losses and gains, DNA rearrangements, and gene mutations [4]. In addition, a growing body of evidence suggests that epigenetic changes such as DNA methylation and histone modification also play crucial roles in hepatocarcinogenesis.

Two seemingly contradictory epigenetic events coexist in cancer: global hypomethylation, which is mainly observed in repetitive sequences throughout the genome, and regional hypermethylation, which is frequently associated with CpG islands within gene promoters [5]. Hypermethylation of CpG islands is a common feature of cancer and is associated with gene silencing. Although the classical two-hit theory posits that tumor suppressor genes are inactivated by gene mutation or deletion, it is now recognized that DNA hypermethylation is a third mechanism by which inactivation of tumor suppressor genes occurs, and that it plays a significant role in tumorigenesis. In contrast to the CpG islands, repetitive DNA elements are normally heavily methylated in somatic tissues. About 45 % of the human genome is composed of repetitive sequences, including long interspersed nuclear elements (LINEs) and short interspersed nuclear element [6], and studies have shown that methylation of such repetitive elements can serve as a surrogate for the global methylcytosine content [7]. In that regard, LINE-1 hypomethylation is known to occur during the development of various human malignancies, including HCC [8, 9].

HCC is generally diagnosed at an advanced stage of tumor progression, and a large fraction of HCC cases are fatal. Thus, a better understanding of the underlying molecular mechanisms and identification of genes critical for early detection of HCC and therapeutic intervention would be highly desirable. Although a number of hyper- or hypomethylated loci have been identified in HCC [10–12], only a few studies have been conducted to unravel the genome-wide methylation status [13–15]. In the present study, we carried out genome-wide CpG island methylation analysis in a set of primary HCC specimens, with and without hepatitis virus infection. We also evaluated the hypomethylation of LINE-1 and assessed its association with aberrant CpG island hypermethylation in HCC.

Materials and methods

Tissue samples and cell lines

A total of 57 primary HCC specimens (HBV-positive, n=21; HCV-positive, n=21; HBV/HCV-negative, n=15) were obtained through surgical resection or needle biopsy at Sapporo Medical University Hospital. Corresponding samples of noncancerous liver tissue were also obtained from 50 patients. HBV surface (HBs) antigen and anti-HCV antibody were measured serologically. An informed consent was obtained from all patients before collection of the specimens. The ten liver cancer cell lines (HT17, PLC/PRF/5, Li-7, huH-1, HuH-7, HepG2, Hep3B, HLE, HLF, and JHH-4) used have been described previously [11]. To analyze restoration of gene expression, cells were treated with 2.0 μM 5-aza-2′-deoxycytidine (5-aza-dC) (Sigma, St Louis, MO, USA) for 72 h, replacing the drug and medium every 24 h. Genomic DNA was extracted using the standard phenol–chloroform procedure. Total RNA was extracted using TRIZOL reagent (Invitrogen, Carlsbad, CA, USA) and then treated with a DNA-free kit (Ambion, Austin, TX, USA). Genomic DNA and total RNA from normal liver tissue from a healthy individual were purchased from BioChain (Hayward, CA, USA).

Methylated CpG island amplification coupled with CpG island microarray

Methylated CpG island amplification (MCA) was performed as described previously [13]. Briefly, 500 ng of genomic DNA was digested with the methylation-sensitive restriction endonuclease *Sma*I (New England Biolabs, Ipswich, MA, USA), after which it was digested with the methylation-insensitive restriction endonuclease *Xma*I. The adaptors were prepared by addition of the oligonucleotides RMCA12 (5′-CCGGGCAGAAAG-3′) and RMCA24 (5′-CCACCGCCATCCGAGCCTTTCTGC-3′). After ligation of the digested DNA to the adaptors, PCR amplification was carried out. Using a BioPrime Plus Array CGH Genomic Labeling System (Invitrogen), MCA amplicons from the HCC samples were labeled with Alexa Fluor 647, while amplicons from a normal liver sample was labeled with Alexa Fluor 555. The labeled MCA amplicons were then hybridized to a custom human CpG island microarray containing 15,134 probes covering 6,157 unique genes (G4497A; Agilent Technologies, Santa Clara, CA, USA) [16]. After washing, the array was scanned using an Agilent DNA Microarray Scanner (Agilent technologies), and the data were processed using Feature Extraction software ver. 10.7 (Agilent Technologies). The data were then analyzed using GeneSpring GX ver. 11 (Agilent Technologies).

Methylation-specific PCR

Genomic DNA (1 μg) was modified with sodium bisulfite using an EpiTect Bisulfite Kit (Qiagen, Hilden, Germany), and methylation-specific PCR (MSP) was performed as described previously [17]. Briefly, PCR was run in a 25-μl

volume containing 50 ng of bisulfite-treated DNA, 1× MSP buffer [67 mM Tris–HCl (pH 8.8), 16.6 mM $(NH4)_2SO_4$, 6.7 mM $MgCl_2$, and 10 mM 2-mercaptoethanol], 1.25 mM dNTP, 0.4 μM each primer, and 0.5 U of JumpStart REDTaq DNA Polymerase (Sigma). The PCR protocol for MSP entailed 5 min at 95°C; 35 cycles of 30 s at 95°C, 30 s at 60°C, and 30 s at 72°C; and a 7 min final extension at 72°C. Primer sequences and PCR product sizes are shown in Supplementary Table 1.

Bisulfite pyrosequencing analysis

Bisulfite pyrosequencing analysis was performed as described previously [17]. The PCR protocol entailed 5 min at 95°C; 45 cycles of 1 min at 95°C, 1 min at 60°C, and 1 min at 72°C; and a 7-min final extension at 72°C. PCR products were then bound to Streptavidin Sepharose beads HP (Amersham Biosciences, Piscataway, NJ); after which, the beads containing the immobilized PCR product were purified, washed, and denatured using a 0.2 M NaOH solution. After addition of 0.3 μM sequencing primer to the purified PCR product, pyrosequencing was carried out using a PSQ96MA system (Qiagen, Hilden, Germany) and Pyro Q-CpG software (Qiagen). Primer sequences and PCR product sizes are shown in Supplementary Table 1.

Quantitative RT-PCR

Single-stranded cDNA was prepared using SuperScript III reverse transcriptase (Invitrogen). Quantitative RT-PCR was carried out using TaqMan Gene Expression Assays (*KLHL35*, Hs00400533_m1; *PAX5*, Hs00172003_m1; *PENK*, Hs00175049_m1; *SPDYA*, Hs00736925_m1; *GAPDH*, Hs99999905_m1; Applied Biosystems, Foster City, CA, USA) and a 7500 Fast Real-Time PCR System (Applied Biosystems) according to the manufacturer's instructions. SDS1.4 software (Applied Biosystems) was used for comparative delta Ct analysis, and *GAPDH* served as an endogenous control.

Statistical analysis

To compare differences in continuous variables between groups, *t* tests or ANOVA with post hoc Tukey's tests were performed. Fisher's exact test or chi-squared test was used for analysis of categorical data. Receiver operator characteristic (ROC) curves were constructed based on the levels of methylation. Values of $P<0.05$ (two-sided) were considered statistically significant. Statistical analyses were carried out using SPSS statistics 18 (IBM Corporation, Somers, NY, USA) and GraphPad Prism ver. 5.0.2 (GraphPad Software, La Jolla, CA, USA).

Results

Genome-wide CpG island methylation analysis in HCC

To screen for CpG island hypermethylation in HCC, we carried out methylated CpG island amplification coupled with CpG island microarray (MCAM) analysis using a set of HCC tissue specimens (HBV-positive, $n=4$; HCV-positive, $n=5$; HBV/HCV-negative, $n=7$). As in an earlier study in which the same array system was used, we utilized a signal ratio (Cy5/Cy3) of >2.0 as the criterion for a methylation-positive probe [13]. The average number of methylated probe sets in the HCC specimens was 566 (range 159–846). To assess the association between hepatitis virus infection and methylation status, we categorized the HCC specimens according to their viral status. The average numbers of methylated probe sets in HBV-positive, HCV-positive, and the HBV/HCV-negative HCC specimens were 574, 598, and 539, respectively, which did not significantly differ ($P=0.840$). Interestingly, however, the numbers of methylated probe sets were more varied among HBV/HCV-negative HCCs, which is indicative of their varied pathological backgrounds (Fig. 1a).

To identify commonly methylated genes in HCC, we selected genes that were methylated in at least two tumors in each group. Among the HBV-positive HCCs, 443 probe sets (corresponding to 332 unique genes) satisfied this criterion. Among the HCV-positive HCCs, 476 probe sets (342 unique genes) satisfied the criterion, and among the HBV/HCV-negative HCCs, 348 probe sets (259 unique genes) satisfied the criterion. Collectively, 714 probes (514 unique genes) were selected as commonly methylated genes. Of those, 137, 146, and 47 probe sets were methylated in only HBV-positive, HCV-positive, or HBV/HCV-negative HCC tissues, respectively (Fig. 1b). By contrast, a large number of genes were methylated in multiple categories, and 169 probe sets were methylated in all three groups (Fig. 1b). Consistent with the above results, unsupervised hierarchical clustering analysis demonstrated that some genes were methylated irrespective of the hepatitis virus status, and that HCV-positive HCCs exhibited the largest number of methylated genes (Fig. 1c, Supplementary Fig. 1). Gene ontology analysis of the commonly methylated genes revealed that genes related to "multicellular organismal process," "developmental process," and "system development" are significantly enriched among the methylated genes (Supplementary Table 2). In addition, pathway analysis suggested that some of the methylated genes are involved in differentiation and development (Supplementary Fig. 2).

Identification of novel genes methylated in HCC

Our MCAM analysis suggested that some genes were methylated in a hepatitis virus-specific manner, but a larger

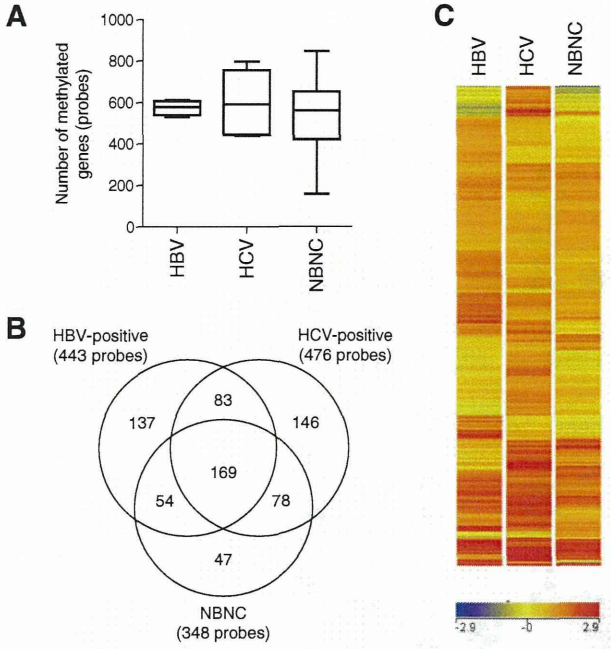

Fig. 1 Genome-wide analysis of CpG island methylation. **a** MCAM analysis was carried out using a series of HCC tissue specimens (HBV-positive, $n=4$; HCV-positive, $n=5$; HBV/HCV-negative, NBNC, $n=7$). MCAM data were categorized into three groups based on the hepatitis virus status, and the numbers of methylated genes in the respective categories are shown. **b** Venn diagram analysis of the methylated genes in the indicated categories. **c** Gene tree view of the MCAM analysis results. A set of 714 probes (514 unique genes) were selected as commonly methylated genes, after which, hierarchical clustering was performed. Each row represents a single probe

number were commonly methylated in HCC. Because recent studies have suggested that aberrant DNA methylation could be a useful diagnostic marker for HCC, we next aimed to identify novel genes frequently methylated in HCC. Among the genes commonly methylated irrespective of hepatitis virus status, we selected 14 (*KLHL35*, *PAX5*, *PENK*, *SPDYA*, *LTBP2*, *DLX1*, *PGBD1*, *WNT9A*, *ADRA1A*, *RHOBTB1*, *GDNF*, *WNT11*, *MLL*, and *PLEC1*) and carried out MSP to assess their methylation status in a series of HCC cell lines (Supplementary Fig. 3). We found that four (*KLHL35*, *PAX5*, *PENK*, and *SPDYA*) of the genes were frequently methylated in HCC cell lines, but showed only little or no methylation in normal liver tissue from a healthy individual (Supplementary Fig. 3). We therefore used quantitative bisulfite pyrosequencing to further analyze the methylation levels of these four genes (Supplementary Figs. 4 and 5).

To determine the extent to which these genes are aberrantly methylated in primary tumors, we analyzed a set of primary HCC specimens (HBV-positive, $n=21$; HCV-positive, $n=21$; HBV/HCV-negative, $n=15$) and corresponding noncancerous liver tissues from the same patients (HBV-positive, $n=18$; HCV-positive, $n=18$; HBV/HCV-negative, $n=14$). Bisulfite pyrosequencing analysis revealed the methylation levels of the four genes to be significantly higher in tumor tissues than in their noncancerous counterparts (*KLHL35*, 37.9 vs. 10.4 %, $P<0.001$; *PAX5*, 23.4 vs. 7.7 %, $P<0.001$; *PENK* 41.1 vs. 22.0 %, $P<0.001$; *SPDYA*, 49.7 vs. 19.3 %, $P<0.001$) (Supplementary Fig. 6). Moreover, these genes were frequently methylated in HCCs, irrespective of the hepatitis virus infection (*KLHL35*, HBV-positive, 37.5 vs. 9.9 %, $P<0.001$; HCV-positive, 38.3 vs. 9.0 %, $P<0.001$; HBV/HCV-negative, 37.7 vs. 13.0 %, $P<0.001$; *PAX5*, HBV-positive, 22.2 vs. 7.6 %, $P=0.014$; HCV-positive, 26.5 vs. 7.2 %, $P<0.001$; HBV/HCV-negative, 20.7 vs. 8.5 %, $P=0.017$; *PENK*, HBV-positive, 45.1 vs. 20.9 %, $P<0.001$; HCV-positive, 39.2 vs. 23.5 %, $P=0.001$; HBV/HCV-negative, 38.2 vs. 21.3 %, $P=0.006$; *SPDYA*, HBV-positive, 51.5 vs. 19.8 %, $P<0.001$; HCV-positive, 46.6 vs. 15.3 %, $P<0.001$; HBV/HCV-negative, 51.3 vs. 23.7 %, $P<0.001$) (Fig. 2a). The association between the methylation of each gene and the clinicopathological features are shown in Table 1. Methylation of *KLHL35* and *PAX5* was correlated with greater age, and *SPDYA* methylation was moderately correlated with higher PIVKA-II levels, but we found no other significant correlations (Table 1). We also generated an ROC curve and observed that methylation of the four genes discriminated strongly between tumor tissues and noncancerous liver tissue, suggesting that methylation of these genes could be a useful tumor marker (Fig. 2b). The most discriminating cutoffs for *KLHL35*, *PAX5*, *PENK*, and *SPDYA* were 14.8 % (sensitivity, 82.5 %; specificity, 88.0 %), 12.5 % (sensitivity, 63.2 %; specificity, 94.0 %), 28.4 % (sensitivity, 70.2 %; specificity, 96.0 %), and 30.3 % (sensitivity, 86.0 %; specificity, 94.0 %), respectively.

Analysis of *KLHL35*, *PAX5*, *PENK*, and *SPYDA* methylation and expression

We next tested whether methylation of *KLHL35*, *PAX5*, *PENK*, and *SPYDA* was associated with their silencing in HCC. Bisulfite pyrosequencing analysis revealed that the degree to which these genes were methylated varied among the HCC cell lines, but it was always much higher than in normal liver tissue from a healthy individual (Fig. 3a). Quantitative RT-PCR analysis confirmed an inverse relationship between methylation and expression of *KLHL35*

Fig. 2 Quantitative methylation analysis of the genes identified by MCAM. **a** Summary of the bisulfite pyrosequencing analysis of *KLHL35*, *PAX5*, *PENK*, and *SPDYA* in tumor tissue (*T*) and noncancerous liver tissue (*N*) from HBV-positive, HCV-positive, and HBV/HCB-negative (NBNC) HCC patients. **b** ROC curve analysis of the methylation of the indicated genes. The area under the ROC curve (*AUC*) for each site conveys its utility (in terms of sensitivity and specificity) for distinguishing between HCC tissue and corresponding noncancerous liver tissue from the same HCC patients

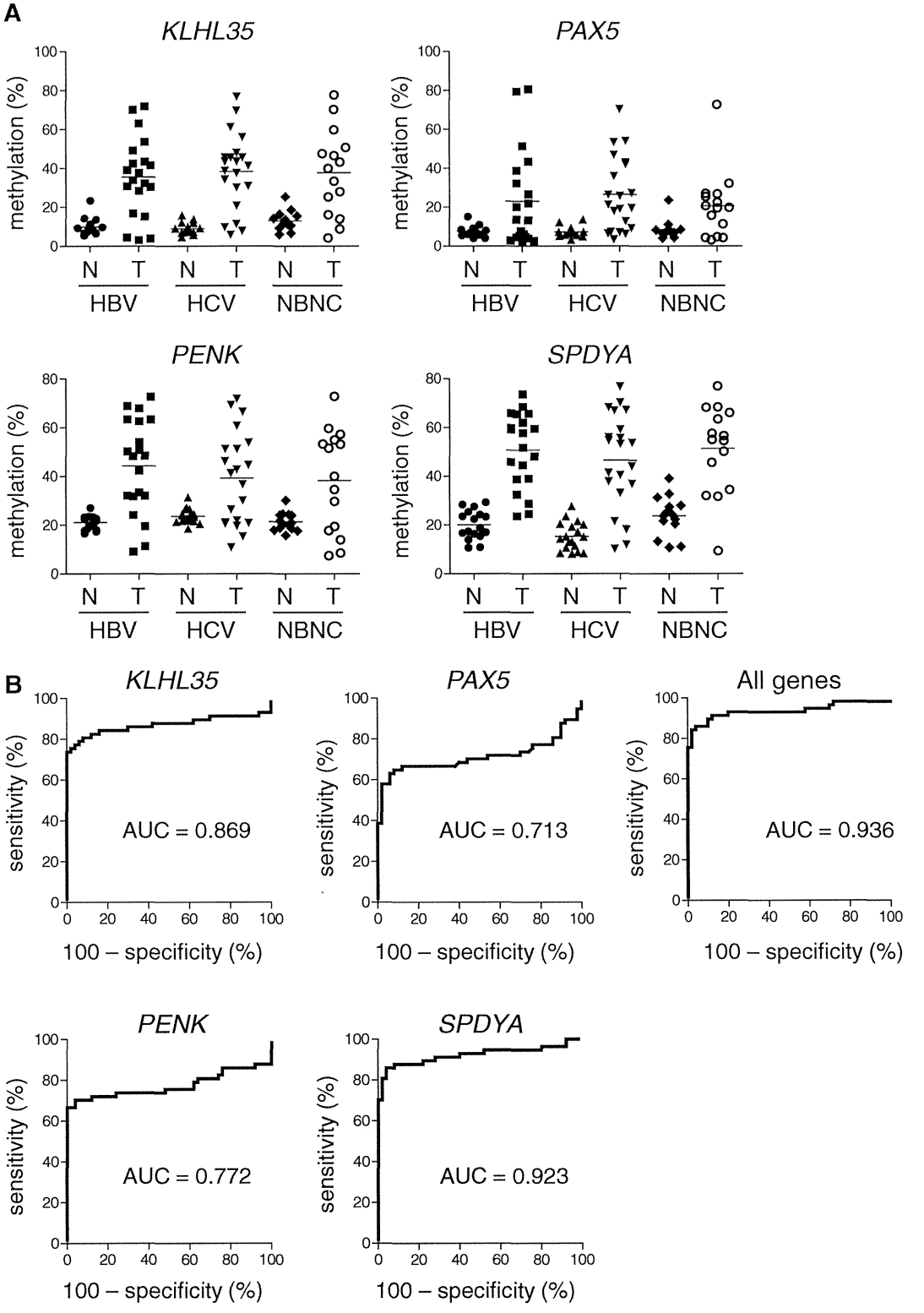

and *PAX5* in the cell lines and normal liver tissue (Fig. 3b), whereas methylation of *PENK* and *SPDYA* did not correlate significantly with their expression levels. The expression of *PENK* was undetectable in seven HCC cell lines and in

Table 1 Association between clinicopathological features and DNA methylation in HCC

	N	*KLHL35* methylation			*PAX5* methylation			*PENK* methylation			*SPDYA* methylation			LINE-1 methylation		
		Mean	SD	*P* value	Mean	SD	*P* value	Mean	SD	*P* value	Mean	SD	*P* value	Mean	SD	*P* value
Age																
≤63	24	30.3	17.7	0.003	18.3	17.1	0.026	41.7	19.3	0.583	51.2	17.9	0.945	49.4	14.8	0.571
>64	23	47.2	18.5		32.3	24.1		44.8	19.6		50.9	15.0		47.2	10.6	
Sex																
M	39	37.5	20.3		22.6	20.9		40.2	19.6		50.1	18.1		47.8	13.3	
F	18	37.2	22.0	0.953	25.2	19.9	0.652	43.1	19.6	0.602	48.7	16.7	0.771	51.5	12.0	0.318
Virus																
HBV	21	35.6	20.3		23.1	24.5		44.3	19.4		50.7	15.4		50.4	13.9	
HCV	21	38.3	19.5		26.5	19.0		39.2	18.8		46.6	19.6		50.2	12.2	
NBNC	15	36.1	22.2	0.900	20.7	17.2	0.698	38.2	21.0	0.603	51.3	18.0	0.668	44.7	12.9	0.359
Child-Pugh																
A	44	39.2	20.0		25.5	22.3		43.4	19.6		51.4	15.6		48.6	12.4	
B	3	29.7	18.2	0.426	19.9	11.8	0.672	41.0	17.1	0.842	45.3	29.5	0.536	44.6	20.6	0.609
PIVKA-II (mAU/ml)																
≤21	16	40.0	19.5		24.0	25.7		42.1	19.1		53.5	14.1		48.0	11.5	
22–66	16	35.8	11.8		23.4	14.2		44.6	14.0		42.9	15.9		52.9	10.7	
>67	15	40.1	26.9	0.795	28.3	24.8	0.802	42.8	24.9	0.933	57.1	16.6	0.039	43.8	15.1	0.136
AFP (ng/ml)																
≤7.4	16	39.3	19.3		25.8	24.1		41.4	19.0		49.4	17.0		47.4	9.2	
7.5–55.0	16	44.9	20.2		31.1	23.2		51.5	15.6		55.0	16.7		50.6	13.4	
>55.1	15	31.1	18.7	0.150	18.1	16.3	0.256	36.3	21.0	0.078	48.7	15.8	0.509	46.9	15.7	0.695
Cirrhosis																
0	27	35.3	23.4		22.2	22.2		40.0	22.1		51.8	18.2		47.7	14.7	
1	24	40.7	16.5	0.353	25.7	20.3	0.559	44.2	17.8	0.467	50.5	15.8	0.795	49.2	11.3	0.687
Vascular invasion																
0	42	38.3	18.5		24.0	21.0		43.9	19.5		52.3	15.1		48.2	12.8	
1	9	35.7	28.9	0.353	23.1	23.3	0.559	33.1	21.5	0.467	46.1	24.2	0.795	49.3	15.1	0.687
TNM stage																
1	6	29.5	15.4		15.0	9.8		50.6	12.1		43.3	20.8		58.4	11.8	
2	20	37.7	20.4		24.6	20.3		44.7	19.3		53.7	11.8		47.5	13.2	
3	13	45.4	14.3		24.4	23.4		43.0	19.3		55.5	13.8		44.8	10.6	
4	6	32.4	28.6	0.335	30.9	28.4	0.639	29.4	23.3	0.262	41.6	25.5	0.181	47.5	16.1	0.200
Multiple cancer																
0	33	38.3	22.1		26.2	23.9		43.9	20.8		51.1	18.5		48.8	14.2	
1	13	38.6	14.3	0.964	22.4	16.9	0.609	41.7	16.4	0.732	50.5	10.7	0.911	48.3	8.5	0.916

NBNC HBV/HCV-negative

normal liver tissue, irrespective of the methylation status (Fig. 3b). Conversely, although *SPDYA* was highly methylated in a majority of HCC cell lines, its expression was detectable in all cells, and most of the HCC lines exhibited greater *SPDYA* expression than did normal liver tissue (Fig. 3b). The above results suggest that *KLHL35* and *PAX5* are epigenetically silenced in HCC cells. Consistent with that idea, treating methylated cell lines with a DNA methyltransferase inhibitor, 5-aza-dC, restored the expression of *KLHL35* and *PAX5* (Fig. 3c). On the other hand, the expression of *PENK* and *SPDYA* does not appear to be affected by methylation.

Analysis of LINE-1 methylation and its association with gene hypermethylation

It was previously reported that LINE-1 is frequently hypomethylated in HCC, though most of those studies focused on HBV-positive tumors. Similarly, by using the bisulfite

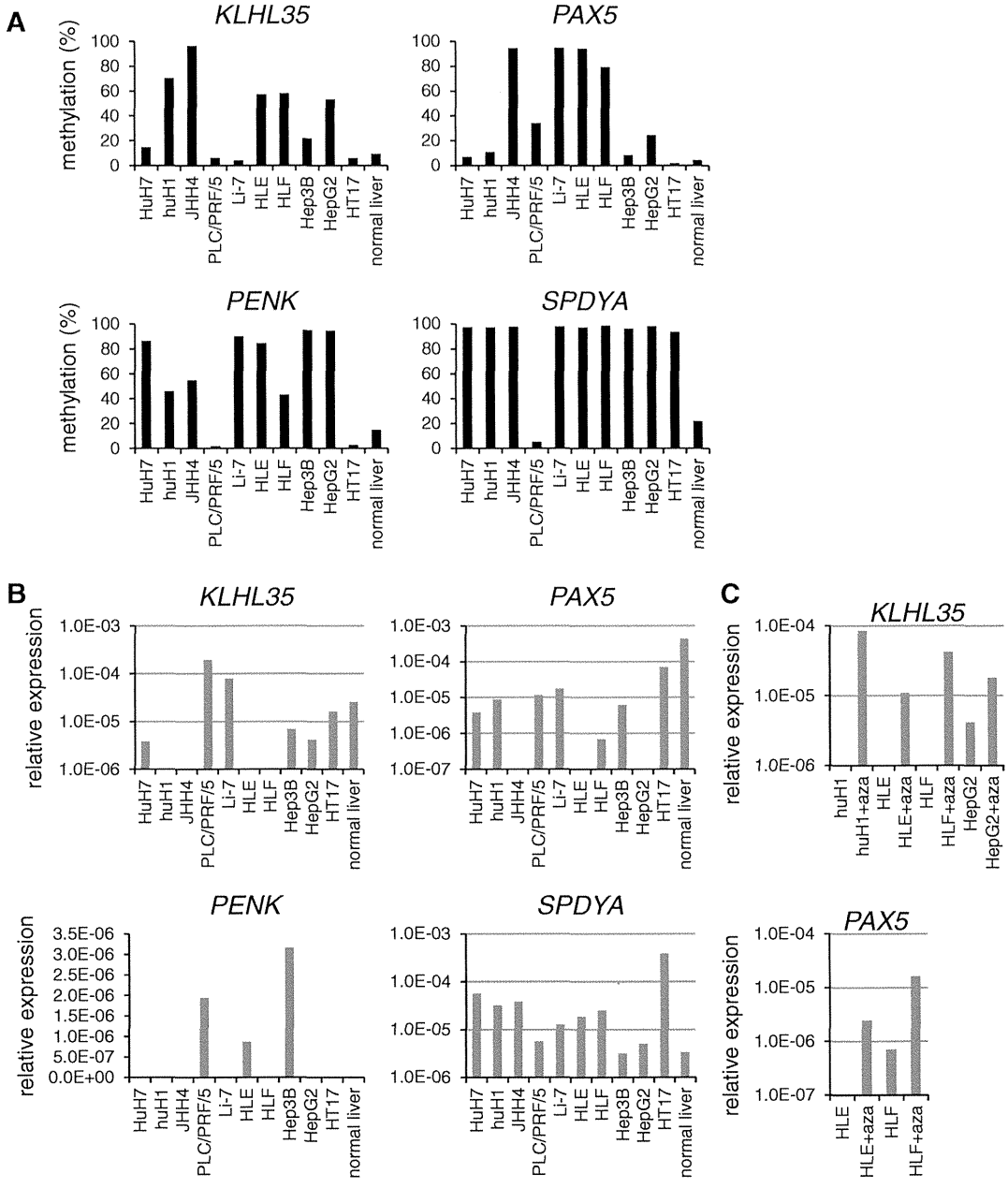

Fig. 3 Analysis of the methylation and expression of the indicated genes in HCC cell lines. **a** Bisulfite pyrosequencing of *KLHL35*, *PAX5*, *PENK*, and *SPDYA* in HCC cell lines and normal liver tissue from a healthy individual. **b** Quantitative RT-PCR of the four genes in HCC cell lines and normal liver tissue. **c** Quantitative RT-PCR of *KLHL35* and *PAX5* in HCC cell lines, with and without 5-aza-dC (*aza*) treatment

pyrosequencing, we found that levels of LINE-1 methylation were significantly lower in tumor tissues than in their noncancerous counterparts (48.5 vs. 66.8 %, $P<0.001$). LINE-1 hypomethylation was prevalent, regardless of the tumor's hepatitis virus status, but the average methylation level was lowest in the HBV/HCV-negative tumors (HBV-positive, 50.8 vs. 66.3 %, $P<0.001$; HCV-positive, 48.9 vs. 67.4 %, $P<0.001$; HBV/HCV-negative, 44.7 vs. 66.6 %, $P<0.001$; Fig. 4a). The ROC curve analysis revealed that LINE-1 methylation discriminated strongly between HCC tissue and noncancerous liver tissue (Fig. 4b), though no significant correlation was found between the levels of LINE-1 methylation and the clinicopathological characteristics of the samples (Table 1). Finally, we tested whether LINE-1 hypomethylation is linked to gene hypermethylation. We found an inverse relationship between the level of

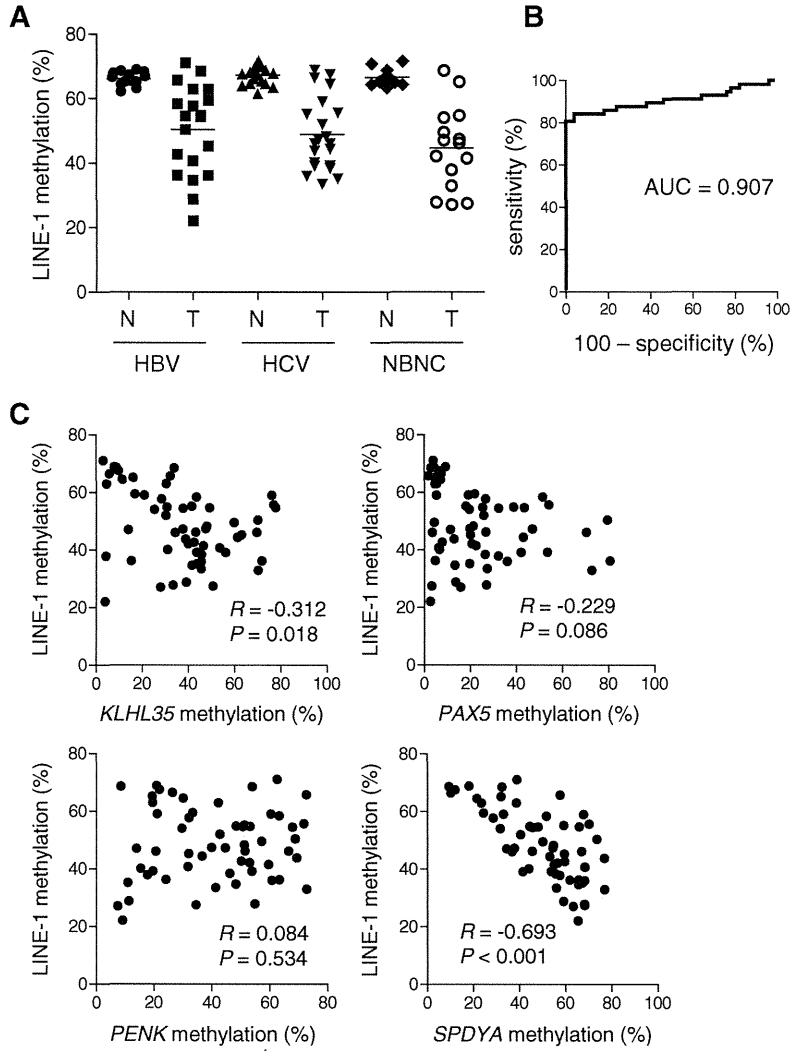

Fig. 4 Analysis of LINE-1 methylation and its association with CpG island hypermethylation in HCC. **a** Summary of bisulfite pyrosequencing analysis of LINE-1 in tumor tissue (*T*) and corresponding noncancerous liver tissue (*N*) from HBV-positive, HCV-positive, and HBV/HCB-negative (*NBNC*) HCC patients. **b** ROC curve analysis of the utility of LINE-1 methylation for distinguishing between HCC tissue and corresponding noncancerous liver tissue from the same HCC patients. **c** Correlation between the level of LINE-1 methylation and methylation of the indicated genes in HCC tissues. The Pearson correlation coefficients and *P* values are shown

LINE-1 methylation and levels of *KLHL35* and *SPDYA* methylation. On the other hand, we found no significant correlation between the LINE-1 hypomethylation and *PAX5* or *PENK* methylation (Fig. 4c).

Discussion

In the present study, we carried out high-throughput CpG island methylation profiling in a set of primary HCC tissues with and without hepatitis virus infection. MCAM analysis enabled us to evaluate the methylation status of more than 6,000 gene promoters with high specificity and sensitivity [13]. Consistent with earlier studies that showed methylation to be more abundant in the HCV-positive HCCs than in the HBV-positive or hepatitis virus-negative HCCs [15, 18], we observed the highest number of methylated genes in HCV-positive HCC tissue. However, we also noted that a large number of genes were commonly methylated among HCCs, irrespective of the hepatitis virus status, indicating that aberrant methylation of multiple genes may be involved in a common mechanism underlying hepatocarcinogenesis. Moreover, studies have also shown that aberrant methylation detected in tissues or blood samples could be a useful biomarker for early detection of HCC [19, 20]. We therefore validated the methylation status of 14 genes and identified four genes that were frequently methylated in HCC tissues but showed little or no methylation in surrounding noncancerous tissues. The high-tumor specificity suggests that methylation of these genes may not occur at precancerous stages, such as chronic hepatitis or liver cirrhosis; instead, they may be acquired during malignant transformation.

The paired box 5 (*PAX5*) gene is a member of the paired box-containing family of transcription factors, which are involved in the control of organ development and tissue differentiation [21]. PAX5 is also known to be a B cell-

specific activator protein that plays an essential role during B cell differentiation, neural development, and spermatogenesis. Methylation of the CpG island of *PAX5* was first discovered in breast cancer cells using the MCA technique [22]. Subsequently, methylation and downregulation of *PAX5* were found in lymphoid neoplasms [23]. In addition, while we are preparing the present manuscript, methylation of *PAX5* was reported in HCC and gastric cancer [24, 25]. Restoration of *PAX5* expression in HCC cells induced growth arrest and apoptosis through upregulation of various target genes, including p53, p21, and Fas ligand, suggesting that the PAX5 acts as a tumor suppressor [24].

The involvement of the kelch-like 35 (*KLHL35*) gene in cancer had not been reported until recently, when a genome-wide analysis of DNA methylation in renal cell carcinoma identified frequent hypermethylation of nine genes, including *KHLH35* [26]. Although the function of the gene product remains unknown, RNAi-induced knockdown of *KHLH35* in HEK293 cells promoted anchorage-independent growth, indicating its possible role in tumorigenesis [26].

The proenkephalin (*PENK*) gene encodes preproenkephalin, a precursor protein that is proteolytically cleaved to produce the endogenous opioid peptides met- and leu-enkephalin. Methylation of the CpG island of *PENK* was first identified in pancreatic cancer cells using the MCA technique [27]. Downregulated expression of *PENK* has also been reported in prostate cancer, suggesting its possible involvement in cancer development [28], and *PENK* methylation was recently identified in lung cancer, bladder cancer, and meningioma [29–31]. Although its functional role in cancer is not fully understood, a recent study showed that in response to cellular stress, PENK physically associates with p53 and RelA (p65) and regulates stress-induced apoptosis [32].

The *SPDYA* encodes Spy1, also known as Speedy, an atypical CDK activator known to promote cell survival, prevent apoptosis, and inhibit checkpoint activation in response to DNA damage [33]. The expression of *SPDYA* is upregulated in breast cancer [34], and its overexpression in a mouse model has been shown to accelerate mammary tumorigenesis [35]. Moreover, a recent study showed overexpression of *SYPDA* in HCC and its association with poor prognosis [36]. These results strongly suggest its involvement in oncogenesis. In the present study, we also observed that most of the HCC cell lines tested exhibited greater expression of *SPDYA* than normal liver tissue, regardless of the methylation status. Among the three transcription variants of *SPDYA* annotated in the NCBI Reference Sequence database, transcription start sites of variants 1 and 3 are located within the CpG island, while that of variant 2 are located approximately 5 kb downstream of the CpG island. Thus, the *SPDYA* transcript in HCC cells may be derived from the downstream transcription start site.

By analyzing the LINE-1 methylation levels, we and others have shown that global hypomethylation is a commonly observed feature of HCC [8, 9, 37]. Earlier studies have suggested that the association between global methylation and hepatitis status may be attributable to hepatitis B virus X protein, which can induce aberrant methylation of specific genes and global hypomethylation [38]. By contrast, we found in the present study that LINE-1 hypomethylation is prevalent among HCC tissues, regardless of the hepatitis virus infection, which suggests that global hypomethylation is involved in a common mechanism underlying hepatocarcinogenesis. It has been shown that the timing of global hypomethylation differs among tumor types. For example, hypomethylation is often observed during the early stages of colorectal and gastric carcinogenesis. By contrast, LINE-1 hypomethylation appears to be tumor-specific in HCC; it is rarely found in precancerous lesions such as chronic hepatitis or liver cirrhosis [8, 9]. A recent study showed that global hypomethylation is associated with a poorer prognosis in HCC patients [39]. In addition, the levels of serum LINE-1 hypomethylation in HCC patients reportedly correlate with serum HBs antigen status, large tumor size, and advanced tumor stage [40]. This suggests that hypomethylation may not occur at precancerous stages, and that LINE-1 methylation could be a useful biomarker with which to identify HCC and predict its clinical outcome.

The relationship between LINE-1 hypomethylation and CpG island hypermethylation in cancer is controversial. In one study, LINE-1 methylation levels were reduced in HCCs with the CpG island methylator phenotype, indicating a positive correlation between global hypomethylation and CpG island hypermethylation [9]. Another study showed that LINE-1 hypomethylation was positively correlated with hypermethylation of only a few genes (*p16*, *CACNA1G*, and *CDKN1C*), while methylation of a large number of genes showed inverse or no correlation with LINE-1 hypomethylation [12]. In the present study, we found that methylation of *KLHL35* and *SPYDA* correlates positively with LINE-1 hypomethylation, whereas levels of *PAX5* or *PENK* methylation are independent of LINE-1 methylation. These results suggest that the association between CpG island methylation and global hypomethylation may be site specific, and that hypomethylation of LINE-1 is a more generalized phenomenon than hypermethylation of CpG islands in HCC.

In summary, by screening targets of DNA methylation in HCC, we identified four frequently methylated genes. These genes are methylated in a cancer-specific manner and could be useful molecular markers for diagnosing HCC. In addition, we observed prevalent LINE-1 hypomethylation in HCC, irrespective of hepatitis virus infection. Identification of aberrant methylation in HCC may provide valuable information that not only contributes to our understanding of the pathogenesis

of the disease, but also to the development of new strategies for diagnosis and therapy.

Acknowledgments We thank Dr. Yutaka Kondo for technical advice on MCAM analysis and Masami Ashida for technical assistance. This study was supported in part by a Grant-in-Aid for Scientific Research (B) from the Japan Society for Promotion of Science (Y. Shinomura), a Grant-in-Aid for the Third-term Comprehensive 10-year Strategy for Cancer Control (M. Toyota and H. Suzuki), and a Grant-in-Aid for Cancer Research from the Ministry of Health, Labor, and Welfare, Japan (M. Toyota and H. Suzuki).

Conflicts of interest None

References

1. Parkin DM, Bray F, Ferlay J, Pisani P. Global cancer statistics, 2002. CA Cancer J Clin. 2005;55:74–108.
2. Chen CJ, Yu MW, Liaw YF. Epidemiological characteristics and risk factors of hepatocellular carcinoma. J Gastroenterol Hepatol. 1997;12:S294–308.
3. Montesano R, Hainaut P, Wild CP. Hepatocellular carcinoma: from gene to public health. J Natl Cancer Inst. 1997;89:1844–51.
4. Thorgeirsson SS, Grisham JW. Molecular pathogenesis of human hepatocellular carcinoma. Nat Genet. 2002;31:339–46.
5. Jones PA, Baylin SB. The fundamental role of epigenetic events in cancer. Nat Rev Genet. 2002;3:415–28.
6. Cordaux R, Batzer MA. The impact of retrotransposons on human genome evolution. Nat Rev Genet. 2009;10:691–703.
7. Yang AS, Estecio MR, Doshi K, Kondo Y, Tajara EH, Issa JP. A simple method for estimating global DNA methylation using bisulfite PCR of repetitive DNA elements. Nucleic Acids Res. 2004;32:e38.
8. Takai D, Yagi Y, Habib N, Sugimura T, Ushijima T. Hypomethylation of line1 retrotransposon in human hepatocellular carcinomas, but not in surrounding liver cirrhosis. Jpn J Clin Oncol. 2000;30:306–9.
9. Kim MJ, White-Cross JA, Shen L, Issa JP, Rashid A. Hypomethylation of long interspersed nuclear element-1 in hepatocellular carcinomas. Mod Pathol. 2009;22:442–9.
10. Kaneto H, Sasaki S, Yamamoto H, Itoh F, Toyota M, Suzuki H, Ozeki I, Iwata N, Ohmura T, Satoh T, Karino Y, Toyota J, Satoh M, Endo T, Omata M, Imai K. Detection of hypermethylation of the p16(ink4a) gene promoter in chronic hepatitis and cirrhosis associated with hepatitis B or C virus. Gut. 2001;48:372–7.
11. Takagi H, Sasaki S, Suzuki H, Toyota M, Maruyama R, Nojima M, Yamamoto H, Omata M, Tokino T, Imai K, Shinomura Y. Frequent epigenetic inactivation of sfrp genes in hepatocellular carcinoma. J Gastroenterol. 2008;43:378–89.
12. Lee HS, Kim BH, Cho NY, Yoo EJ, Choi M, Shin SH, Jang JJ, Suh KS, Kim YS, Kang GH. Prognostic implications of and relationship between CpG island hypermethylation and repetitive DNA hypomethylation in hepatocellular carcinoma. Clin Cancer Res. 2009;15:812–20.
13. Gao W, Kondo Y, Shen L, Shimizu Y, Sano T, Yamao K, Natsume A, Goto Y, Ito M, Murakami H, Osada H, Zhang J, Issa JP, Sekido Y. Variable DNA methylation patterns associated with progression of disease in hepatocellular carcinomas. Carcinogenesis. 2008;29:1901–10.
14. Arai E, Ushijima S, Gotoh M, Ojima H, Kosuge T, Hosoda F, Shibata T, Kondo T, Yokoi S, Imoto I, Inazawa J, Hirohashi S, Kanai Y. Genome-wide DNA methylation profiles in liver tissue at the precancerous stage and in hepatocellular carcinoma. Int J Cancer. 2009;125:2854–62.
15. Deng YB, Nagae G, Midorikawa Y, Yagi K, Tsutsumi S, Yamamoto S, Hasegawa K, Kokudo N, Aburatani H, Kaneda A. Identification of genes preferentially methylated in hepatitis C virus-related hepatocellular carcinoma. Cancer Sci. 2010;101:1501–10.
16. Goto Y, Shinjo K, Kondo Y, Shen L, Toyota M, Suzuki H, Gao W, An B, Fujii M, Murakami H, Osada H, Taniguchi T, Usami N, Kondo M, Hasegawa Y, Shimokata K, Matsuo K, Hida T, Fujimoto N, Kishimoto T, Issa JP, Sekido Y. Epigenetic profiles distinguish malignant pleural mesothelioma from lung adenocarcinoma. Cancer Res. 2009;69:9073–82.
17. Suzuki H, Yamamoto E, Nojima M, Kai M, Yamano HO, Yoshikawa K, Kimura T, Kudo T, Harada E, Sugai T, Takamaru H, Niinuma T, Maruyama R, Yamamoto H, Tokino T, Imai K, Toyota M, Shinomura Y. Methylation-associated silencing of microrna-34b/c in gastric cancer and its involvement in an epigenetic field defect. Carcinogenesis. 2010;31:2066–73.
18. Nishida N, Nagasaka T, Nishimura T, Ikai I, Boland CR, Goel A. Aberrant methylation of multiple tumor suppressor genes in aging liver, chronic hepatitis, and hepatocellular carcinoma. Hepatology. 2008;47:908–18.
19. Wong IH, Zhang J, Lai PB, Lau WY, Lo YM. Quantitative analysis of tumor-derived methylated p16ink4a sequences in plasma, serum, and blood cells of hepatocellular carcinoma patients. Clin Cancer Res. 2003;9:1047–52.
20. Zhang YJ, Wu HC, Shen J, Ahsan H, Tsai WY, Yang HI, Wang LY, Chen SY, Chen CJ, Santella RM. Predicting hepatocellular carcinoma by detection of aberrant promoter methylation in serum DNA. Clin Cancer Res. 2007;13:2378–84.
21. Carotta S, Holmes ML, Pridans C, Nutt SL. Pax5 maintains cellular identity by repressing gene expression throughout B cell differentiation. Cell Cycle. 2006;5:2452–6.
22. Palmisano WA, Crume KP, Grimes MJ, Winters SA, Toyota M, Esteller M, Joste N, Baylin SB, Belinsky SA. Aberrant promoter methylation of the transcription factor genes pax5 alpha and beta in human cancers. Cancer Res. 2003;63:4620–5.
23. Lazzi S, Bellan C, Onnis A, De Falco G, Sayed S, Kostopoulos I, Onorati M, D'Amuri A, Santopietro R, Vindigni C, Fabbri A, Righi S, Pileri S, Tosi P, Leoncini L. Rare lymphoid neoplasms coexpressing B- and T-cell antigens. The role of pax-5 gene methylation in their pathogenesis. Hum Pathol. 2009;40:1252–61.
24. Liu W, Li X, Chu ES, Go MY, Xu L, Zhao G, Li L, Dai N, Si J, Tao Q, Sung JJ, Yu J. Paired box gene 5 is a novel tumor suppressor in hepatocellular carcinoma through interaction with p53 signaling pathway. Hepatology. 2011;53:843–53.
25. Li X, Cheung KF, Ma X, Tian L, Zhao J, Go MY, Shen B, Cheng AS, Ying J, Tao Q, Sung JJ, Kung HF, Yu J. Epigenetic inactivation of paired box gene 5, a novel tumor suppressor gene, through direct upregulation of p53 is associated with prognosis in gastric cancer patients. Oncogene. 2011. doi:10.1038/onc.2011.511.
26. Morris MR, Ricketts CJ, Gentle D, McRonald F, Carli N, Khalili H, Brown M, Kishida T, Yao M, Banks RE, Clarke N, Latif F, Maher ER. Genome-wide methylation analysis identifies epigenetically inactivated candidate tumour suppressor genes in renal cell carcinoma. Oncogene. 2011;30:1390–401.
27. Ueki T, Toyota M, Skinner H, Walter KM, Yeo CJ, Issa JP, Hruban RH, Goggins M. Identification and characterization of differentially methylated cpg islands in pancreatic carcinoma. Cancer Res. 2001;61:8540–6.
28. Goo YA, Goodlett DR, Pascal LE, Worthington KD, Vessella RL, True LD, Liu AY. Stromal mesenchyme cell genes of the human prostate and bladder. BMC Urol. 2005;5:17.

29. Chung JH, Lee HJ, Kim BH, Cho NY, Kang GH. DNA methylation profile during multistage progression of pulmonary adenocarcinomas. Virchows Arch. 2011;459:201–11.
30. Chung W, Bondaruk J, Jelinek J, Lotan Y, Liang S, Czerniak B, Issa JP. Detection of bladder cancer using novel DNA methylation biomarkers in urine sediments. Cancer Epidemiol Biomarkers Prev. 2011;20:1483–91.
31. Kishida Y, Natsume A, Kondo Y, Takeuchi I, An B, Okamoto Y, Shinjo K, Saito K, Ando H, Ohka F, Sekido Y, Wakabayashi T. Epigenetic subclassification of meningiomas based on genome-wide DNA methylation analyses. Carcinogenesis. 2012;33:436–41.
32. McTavish N, Copeland LA, Saville MK, Perkins ND, Spruce BA. Proenkephalin assists stress-activated apoptosis through transcriptional repression of nf-kappab- and p53-regulated gene targets. Cell Death Differ. 2007;14:1700–10.
33. Gastwirt RF, McAndrew CW, Donoghue DJ. Speedy/ringo regulation of CDKs in cell cycle, checkpoint activation and apoptosis. Cell Cycle. 2007;6:1188–93.
34. Zucchi I, Mento E, Kuznetsov VA, Scotti M, Valsecchi V, Simionati B, Vicinanza E, Valle G, Pilotti S, Reinbold R, Vezzoni P, Albertini A, Dulbecco R. Gene expression profiles of epithelial cells microscopically isolated from a breast-invasive ductal carcinoma and a nodal metastasis. Proc Natl Acad Sci U S A. 2004;101:18147–52.
35. Golipour A, Myers D, Seagroves T, Murphy D, Evan GI, Donoghue DJ, Moorehead RA, Porter LA. The spy1/ringo family represents a novel mechanism regulating mammary growth and tumorigenesis. Cancer Res. 2008;68:3591–600.
36. Ke Q, Ji J, Cheng C, Zhang Y, Lu M, Wang Y, Zhang L, Li P, Cui X, Chen L, He S, Shen A. Expression and prognostic role of spy1 as a novel cell cycle protein in hepatocellular carcinoma. Exp Mol Pathol. 2009;87:167–72.
37. Lin CH, Hsieh SY, Sheen IS, Lee WC, Chen TC, Shyu WC, Liaw YF. Genome-wide hypomethylation in hepatocellular carcinogenesis. Cancer Res. 2001;61:4238–43.
38. Park IY, Sohn BH, Yu E, Suh DJ, Chung YH, Lee JH, Surzycki SJ, Lee YI. Aberrant epigenetic modifications in hepatocarcinogenesis induced by hepatitis B virus X protein. Gastroenterology. 2007;132:1476–94.
39. Calvisi DF, Simile MM, Ladu S, Pellegrino R, De Murtas V, Pinna F, Tomasi ML, Frau M, Virdis P, De Miglio MR, Muroni MR, Pascale RM, Feo F. Altered methionine metabolism and global DNA methylation in liver cancer: relationship with genomic instability and prognosis. Int J Cancer. 2007;121:2410–20.
40. Tangkijvanich P, Hourpai N, Rattanatanyong P, Wisedopas N, Mahachai V, Mutirangura A. Serum line-1 hypomethylation as a potential prognostic marker for hepatocellular carcinoma. Clin Chim Acta. 2007;379:127–33.

特集
胆と膵 Vol. 34 (2) p. 143～148, 2013
胆道癌，膵癌に対する個別化治療の新展開

ゲノムワイド関連解析による ジェムシタビン副作用関連遺伝子の同定

前佛　均[1]・清谷　一馬[2]・宇野　智子[3]・木村　康利[3]
薙田　泰誠[2]・光畑　直喜[4]・伊奈志乃美[5]・鬼原　史[3]
山上　裕機[5]・平田　公一[3]・中村　祐輔[1]

要約：抗癌剤による副作用発現の有無は多くの要因が関係して規定されているものと考えられるが，遺伝的要因もその重要な因子の一つと考えられている。われわれはジェムシタビンにより引き起こされる重篤な骨髄抑制と関連する遺伝子多型（一塩基多型：SNP）を同定するため，164例のジェムザール単剤治療症例を用いてゲノムワイド関連解析および再現性確認のためのreplication studyを行った。その結果ジェムシタビンによる副作用と強い関連をもつ可能性の高い四つのSNPを含む遺伝領域を同定した（*DAPK1*上のrs11141915：$P=1.27\times10^{-6}$，2q12に存在するrs1901440：$P=3.11\times10^{-6}$，*PDE4B*上のrs12046844：$P=4.56\times10^{-5}$，3q29に存在するrs11719165：$P=5.98\times10^{-5}$）。同定された四つのSNPを用いて副作用リスクに働くと考えられるgenotypeの合計数に応じて各症例を点数化したところ，点数の高い症例では低い症例に比べて有意に副作用の発現率が高くなることが示された。今回同定された四つの遺伝子多型を用いたスコアリングシステムはジェムザールによる副作用の投与前診断に有用となる可能性が示された。

Key words：ジェムシタビン，骨髄抑制，ゲノムワイド関連解析，遺伝子多型

はじめに

現在胆膵悪性疾患をはじめ多くの悪性腫瘍に対する治療薬として適応となっているジェムシタビン（ジェムザール®）は骨髄抑制をはじめ，有害事象の発生頻度が決して少なくない薬剤であるが，その副作用の発現を規定する遺伝的要因についてはいまだ十分に解明されていないのが現状である。生命の設計図とも言われる人の遺伝情報（ゲノム配列）は同じ人間といえども個人間でわずかな違いが存在することが知られており，遺伝子多型（一塩基多型）と呼ばれる塩基配列の個人差を比較することで副作用の発現と関係する遺伝子を同定しようとする解析が進んできており，一部は日常臨床に応用されている。近年，ゲノム全体にわたり一塩基多型をgenotypingする技術が進歩し，ゲノムワイド関連解析（genome-wide association study，GWAS：「ジーワス」と呼ばれることが多い）という方法によりこれまで副作用との関連が全く知られていなかった新たな副作用関連遺伝子を発見する試みがなされるようになってきた。ジェムシタビンはSLC28A1，SLC28A3，SLC 29A1などの薬剤輸送タンパクを介して血中から細胞内に入り[1～3]，deoxycyti-

A Genome-wide Association Study Identifies Four Genetic Markers for Hematological Toxicities in Cancer Patients Receiving Gemcitabine Therapy
Hitoshi Zembutsu et al

1）東京大学医科学研究所ヒトゲノム解析センター（〒113-0033 文京区本郷7-3-1）
2）理化学研究所ゲノム医科学研究センター
3）札幌医科大学医学部外科学第一講座
4）呉共済病院泌尿器科
5）和歌山県立医科大学外科学第二講座

dine kinase (dCK), cytidine deaminase (CDA) などの酵素により代謝を受けることが知られていることから[4]，これらの既知遺伝子上の多型と副作用との関係を調べた報告はいくつか存在するが，現在のところ副作用と強い関連を示す遺伝子多型は同定されていない。本研究はゲノムワイド関連解析を通じジェムザールによる副作用と強い関係を有する遺伝子多型を同定することで，副作用予測診断へ応用することを目的として行われた[5]。

Ⅰ．ジェムシタビンによる有害事象

ジェムシタビン単剤による抗腫瘍治療を受けた174症例を対象に解析を行った（表1）。174例中grade 3以上の白血球/好中球減少症をきたした54例をcase，副作用を示さなかった120例をcontrolとしcase-control studyを行った。解析は21例のcaseおよび58例のcontrolをゲノムワイド関連解析（GWAS）に用い，33例のcaseおよび62例のcontrolをGWAS結果の再現性確認のためのreplication studyに用いた。case-control間で有意な性差を認めず（$P>0.64$），年齢分布にも有意差を認めなかった（$P>0.53$）。疾患別では，半分以上の症例が膵癌(56.9%)でその他肺癌(20.1%)，胆管癌（18.4%）などであった。GWASで用いた症例と，再現性確認のためのreplication studyで用いたサンプル間で疾患分布に有意な差を認めなかった。

Ⅱ．ゲノムワイド関連解析によるジェムシタビン副作用関連候補遺伝子の同定

ジェムシタビン投与により骨髄抑制（>grade 3）が認められた21例と，投与により有害事象を認めなかった58例を用いて，ゲノム全体にわたり（約610,000 SNP）遺伝子多型をスクリーニングした。得られた各症例の610,000 SNPのgenotype情報を用いてcase-control関連解析（Fisherの正確検定）を行った。その結果，もっとも副作用と強い関連を示した遺伝子多型（SNP）は$P=0.000006690$を示した。図1にゲノム全体にわたるマーカーSNPとジェムシタビン副作用との関連の強さをグラフで表したもの（マンハッタンプロット）を示すが，ジェムシタビンの副作用と関係するSNPはゲノム全体にわたり散在している可能性を示している。

Ⅲ．ジェムシタビン副作用関連候補遺伝子のreplication study

ゲノムワイド関連解析の結果の再現性を確認するために，有意差上位100 SNPについて33例のcaseおよび62例のcontrolを用いて関連解析を行った。100 SNPに対するreplication studyの結果$P<0.05$を示す4 SNPが同定された（表2）。4 SNPとジェムシタビンによる骨髄抑制との関連はそれぞれ9番染色体上のrs11141915が$P=2.77\times10^{-3}$，2番染色体上のrs1901440は$P=1.82\times10^{-2}$，1番染色体上のrs12046844は$P=3.09\times10^{-2}$，3番染色体上のrs11719165は$P=4.61\times10^{-2}$を示した。さらにこの4 SNPについてGWASで用いたcaseおよびcontrol症例をそれぞれ加えて解析した結果，いずれもゲノムワイド有意水準である1.07×10^{-7}に達するSNPは存在しなかったものの，9番染色体上のrs11141915は$P=1.27\times10^{-6}$，オッズ比4.10（95% CI：2.21-7.62），2番染色体上のrs1901440は$P=3.11\times10^{-6}$，オッズ比34.00（95% CI：4.29-269.48），1番染色体上のrs12046844は$P=4.56\times10^{-5}$，オッズ比4.13(95% CI：2.10-8.14)，3番染色体上のrs11719165は$P=5.98\times10^{-5}$，オッズ比2.60（95% CI：1.63-4.14）を示し，この4 SNPを含む遺伝的領域はジェムシタビンによる骨髄抑制と何らかの関連を示す結果となった。また，4遺伝領域の中で9番染色体上の領域については*DAPK1*，1番染色体上の領域については*PDE4B*という既知の遺伝子を含んでいた。

Ⅳ．遺伝子多型情報を用いたジェムシタビンによる骨髄抑制予測診断モデル

ジェムシタビンによる骨髄抑制と関連が示唆された4SNPはmultiple logistic regression解析の結果それぞれ独立した副作用予測因子であったため，この4SNPを用いた骨髄抑制予測診断システムについて検討を行った。四つのSNPについて骨髄抑制リスクに働くと考えられるgenotypeを持っている場合，それぞれのSNPについて1点を与え，もっていない場合には0点として各症例合計点数別に骨髄抑制発現群（case）と副作用を認めなかった群（control）で分布を調べた結果が表3および図2である。スコア0または1を示した113例中骨髄抑制群は11.5%，スコア2については60.9%，スコア3については86.7%が骨髄抑制発現群が占めており，コントロール群に比べ有意に高いスコ